

Experimental and Theoretical Investigation of CO₂ Adsorption on Amine-Modified Pumice as an Affordable Adsorbent

Avishan, Maryam; Noorpoor, Ali Reza*⁺

School of Environment, College of Engineering, University of Tehran.
P.O. Box 14155-6135 Tehran, I.R. IRAN

Nazari Kudahi, Saeed

Environment Research Department, Niroo Research Institute, P.O.Box 14665/517 Tehran, I.R. IRAN

ABSTRACT: In the present work, experimental and theoretical aspects of CO₂ adsorption on the amine-modified pumice, as a new adsorbent, was investigated. CO₂ adsorption measurements were performed at three different temperatures (298, 328, and 348 K), and pressures up to 1 atm. To determine the best-fitting isotherm, the experimental equilibrium data were analyzed using eight adsorption isotherm models with two and three parameters. Four two-parameter equations, namely the Langmuir, Freundlich, BET, and Temkin, and four three-parameter equations, namely the Redlich-Peterson, Sips, Toth, and Dubinin-Astakhov were used. To evaluate the adequacy of the fitting of the isotherm models, the average relative error was calculated. Furthermore, Henry's law constant for evaluating the adsorption affinity of CO₂ on the adsorbent was estimated by the Virial model. The results showed the modified pumice demonstrated better adsorption at the temperature of 298 K. Its adsorption capacity (0.510 mmol/g) was almost twice as much as that of raw pumice. The Freundlich model, in comparison with the other two-parameter models, and the Sips model, compared to the other three-parameter models, showed the best correspondence with CO₂ adsorption's experimental data, with average relative errors of less than 3% observed at all temperatures. The results suggest that the amount of E (kJ/mol) (the characteristic energy of adsorption D-A isotherm) at 298K and 328K was lower than 8, which indicates the domination of the physical adsorption mechanism in the process of CO₂ adsorption on modified pumice.

KEYWORDS: CO₂ adsorption, Pumice, Adsorption isotherm models, Henry's law constant.

INTRODUCTION

Global warming, which stems from the increase in the emissions of greenhouse gases, and its consequences for

the earth's ecosystem are amongst the biggest challenges mankind is facing in the twenty-first century. Due to

* To whom correspondence should be addressed.

+ E-mail: noorpoor@ut.ac.ir

1021-9986/2021/4/1148-1161

14/\$/6.04

industrialization, carbon dioxide (CO₂) emissions account for around 60% of the effects of global warming [1,2]. Thus, it is necessary to develop and implement new and efficient technologies in order to reduce CO₂ emissions, and there have been good efforts to do so through carbon Capture and Storage (CCS) [3,4]. Several studies have been conducted on the separation processes of CO₂ and they have resulted in methods such as chemical absorption [5,6], adsorption [7,8], and membrane technology [9,10]. In the large-scale separation of CO₂ from the gas flow, the process of adsorption, due to its many advantages, is of particular interest. The advantages include: “low cost, low regeneration energy, ease of handling, fast kinetics, high CO₂ capacity and selectivity” [11-13]. A wide range of adsorbents has been examined, characterized by both physisorption and chemisorption mechanisms [14]. Zeolites, carbonaceous materials, metal-organic frameworks, amine-based solid adsorbents are amongst the suitable adsorbents for CO₂ which have been studied [15,16].

Despite the use of numerous materials as adsorbents for CO₂ capture, their commercial use in industries is costly. An ideal adsorbent should enjoy high adsorption capacity, selectivity, and stability. It also needs to be cost-effective and easy to regenerate. Considering the fact that the adsorption stage accounts for the largest share of costs (70%-90%) in CCS, at the moment, identifying natural adsorbents, which are inexpensive and eco-friendly, and not in need of complex synthesis processes is crucial to the development of CCS [17].

The application of pumice in academic research in the area of environmental engineering could be divided into three categories of water and wastewater, waste, and air treatment. A significant share of the research conducted is into water and wastewater treatment. It includes the efficient use of pumice to remove water hardness and pollutants such as heavy metals and colors [18]. The studies on the use of pumice in the area of air pollution are rare. Two examples of such studies would be the one concerned with removing VOCs using natural materials during composting of poultry litter in 2009 and the one which involved the examination of ethylbenzene adsorption using a method called Catalytic Ozonation Process in 2017 [19, 20]. This rock is inexpensive and easy to access throughout the world and could reduce the process costs considerably. The cellular structure of pumice (porous surface and irregular structure), large surface area,

high porosity (90% on average), and containing -OH groups, make this igneous rock a suitable choice for the adsorption process [21].

In choosing additives for the purpose of modifying the surface of pumice, the constituents of the adsorbent, economic and environmental considerations of the additive, and the modification process, and the final product should be taken into account. Silica is a highly porous solid that is a good choice for modifying chemical compounds to increase the rate of CO₂ adsorption and has been extensively studied [22, 23]. According to the fact that more than 50% of pumice is made of silica, a method of modification using well-explored amine [23] could lead to favorable results in terms of the improvement of pumice adsorption as the base matter. Research suggests that the best amine compound for the selection and adsorption of CO₂ is TEPA [23]. Thus, in this study, pumice and TEPA were chosen as the base matter and the modifying additive, respectively. For and adsorption process to be applied in industries, cyclic adsorption should be considered.

Cyclic adsorption processes such as Pressure Swing Adsorption (PSA), and Temperature Swing Adsorption (TSA) have grabbed attention. PSA and TSA are cyclic adsorption processes with changes in temperature and pressure during adsorption and desorption. In general, the effectiveness of an adsorbent is defined in terms of its capacity, mechanical resistance, sensitivity to regeneration cycles, and reusability [24]. For and adsorption process to be applied in industries, cyclic adsorption should be considered. PSA and TSA are cyclic adsorption processes with changes in temperature and pressure during adsorption and desorption [25]. PSA is used to separate and purify gases and is an economical replacement for traditional adsorption processes. The main feature of this process is the swing between adsorption and desorption following the increase and decrease in pressure, respectively. The effectiveness of PSA depends on the number of adsorption beds, the size of beds, layers, and the structure of the cycle. In practice, a Cyclic Steady State (CSS) is needed for PSA [26].

A normal TSA consists of two adsorption columns with a fixed bed and performs between two various temperatures. While the adsorption process is being done in a column, in the other one regeneration is happening. In the first stage of regeneration, the gas is heated up and

at the end of desorption, the bed cools down (adsorption, desorption, and cooling down). Every TSA process gets close to a cyclic steady state. In this state, conditions at the end and beginning are the same [27].

However, one of the most important characteristics of evaluating an adsorbent is its capacity. Adsorption isotherms [14, 28], which can give information about the adsorption capacity, adsorption mechanism, and the quantitative distribution of the adsorbate on the adsorbent, are used as an essential method to predict and compare the process of adsorption. As a result, the optimization of adsorption mechanisms and efficient design of adsorption systems becomes possible [29-31].

Modeling of the equilibrium experimental data on the adsorption of CO₂ on various adsorbents is very important. Therefore, over the past years, several studies have been conducted in this regard. *Serafin et al.* [16], *Adeloun et al.* [32], *Singh et al.* [33], and *Rashidi et al.* [34] drew on two- and three-parameter isotherms for the adsorption of CO₂ on Activated Carbon (AC). *Adeloun et al.* tested Langmuir, Freundlich, Dubinin-Astakhov, Temkin, Redlich-Peterson, Sips, and Toth isotherms and found that the molecules of CO₂ bind onto the heterogeneous surface of AC in a monolayer pattern and, also that Redlich-Peterson model best fitted the experimental data [32]. In a study carried out by *Rashidi et al.* on commercial Norit® SX2 AC as an adsorbent, the Freundlich isotherm, in comparison to Langmuir, Dubinin-Astakhov, and Temkin models, was shown to perfectly fit the data from experiment [34]. Moreover, *Serafin et al.* used the equations of Langmuir and Dubinin-Astakhov for the adsorption of CO₂ on AC [30]. In addition, *Chowdhury et al.* experimented with the adsorption of CO₂ on graphene under high and low and concluded that the Toth model was the best option [35]. Furthermore, *Noorpoor et al.* used equilibrium modeling to explain CO₂ adsorption on UiO-66 and graphene oxide composite. They coupled Langmuir, Freundlich, BET, Toth, Dubinin-Astakhov, and Maxwell-Stefan models with vacancy solution theory [31].

Thus, the main purpose of this study was to investigate, for the first time, CO₂ adsorption behavior on amine-modified pumice. To do so, eight isotherm models were used, namely the two-parameter models of Langmuir, Freundlich, BET, and Temkin, as well as the three-parameter models of Toth, Sips, Redlich-Peterson, and Dubinin-Astakhov. The goal was to find the best isotherm

equilibrium model with the lowest mean relative error between the model and the experimental data of CO₂ adsorption.

THEORETICAL SECTION

Equilibrium modeling of CO₂ adsorption on raw and modified pumice

Langmuire isotherm model

The Langmuir isotherm model was defined as the most basic model for describing the monolayer adsorption on a homogeneous surface [36]. The Langmuir equation is based on the following assumptions:

- The adsorbent's surface is homogeneous;
- There is no interaction between the adsorbed molecules;
- Molecules are fixed in their places;
- Only one layer of molecules are involved in the process of adsorption;
- The adsorption system is in equilibrium; and
- The adsorption energy remains stable and unchanged on each site [1, 37].

Eq. (1) shows the Langmuir isotherm model:

$$q = \frac{q_m K_L P}{(1 + K_L P)} \quad (1)$$

Where q (mmol/g) is the amount of CO₂ adsorption, q_m (mmol/g) is the maximum monolayer adsorption capacity of the adsorbent, P (kPa) is the CO₂ equilibrium pressure and K_L (1/kPa) is the Langmuir equilibrium constant or the affinity constant [38].

Freundlich isotherm model

The adsorption of molecules on homogeneous surfaces is not very common [37], so it is necessary to have a model to describe non-ideal, reversible, and multilayer adsorption on heterogeneous surfaces. The Freundlich isotherm is the most famous model used to describe such adsorption processes. In this model, the adsorption energy is significantly decreased due to the drop in the number of available adsorption sites [29, 37]. This model is shown in Eq. (2):

$$q = K_f P^{1/n} \quad (2)$$

Where q (mmol/g) is the capacity of adsorption of CO₂ by the adsorbents, K_f is the constant of the Freundlich

isotherm ($\text{mmol/g atm}^{1/n}$), P (kPa) is the CO_2 equilibrium pressure and n is the heterogeneity factor that represents the deviation of the linearity of the adsorption [1,37].

BET isotherm model

In gas-solid systems, which are in equilibrium, in order to describe monolayer and multilayer adsorption, the BET model is used. In this model, it is assumed that the adsorption heat is the same on different layers and equals the condensation heat [29]. Eq. (3) shows the BET isotherm:

$$q = \frac{q_b \cdot K_B \cdot P}{(P - P_0) \left[1 + (K_B - 1) \left(\frac{P}{P_0} \right) \right]} \quad (3)$$

Where q (mmol/g) is the amount of CO_2 adsorbed, q_b (mmol/g) is the maximum loading of CO_2 into the surface of the adsorbent, P (kPa) is the CO_2 equilibrium pressure, P_0 (kPa) is the adsorbate monolayer saturation pressure and K_B (1/kPa) is the BET adsorption isotherm constant [29,39].

Temkin isotherm model

Another isotherm model helping us to explain adsorption on heterogeneous surfaces is the Temkin model. The Temkin model takes into consideration the indirect effects of the interactions between the adsorbate and the adsorbent during the process of adsorption [30]. The adsorption heat (ΔH_{ads}) in each layer decreases linearly. The reason for this decrease is the coverage between the adsorbate and the adsorbent [30,40]. The Temkin isotherm is given below:

$$q = \frac{RT}{b_T} \ln K_T C_e \quad (4)$$

Where $B=RT/b$ with b (J/mol) and K_T (1/atm) as the Temkin constants, T (K) is the temperature and R (8.314 J/mol K) is the universal gas constant[40].

Toth isotherm model

The Toth isotherm model is another experimental equation developed to modify the Langmuir isotherm model by reducing the gap between the predicted and experimental data of the adsorption equilibrium. This model, which is valid for the highest and lowest boundaries of concentration, is useful for systems of heterogeneous adsorption at all pressures. t in this model

signals the heterogeneity of the surface. If $t=1$, the Toth model turns into the Langmuir model[1, 37]. The Toth model is shown below:

$$q = \frac{q_s K_T P}{\left(1 + (K_T P)^t \right)^{1/t}} \quad (5)$$

Where q (mmol/g) indicates the amount of adsorbed CO_2 , q_s (mmol/g) is the saturation loading, P (kPa) is the equilibrium pressure of CO_2 , K_T (1/kPa) is the Toth isotherm's constant which describes the tendency of CO_2 to be adsorbed on the surface of the adsorbent, and t is the parameter signaling the heterogeneity of the adsorbent [29].

Sips isotherm model

This model is a combination of the Freundlich and Langmuir isotherms and is effective for predicting the adsorption process on heterogeneous surfaces. Therefore, it has successfully dealt with the limits, in Freundlich model, regarding the rise in the concentration of the adsorbate. When the concentration of the adsorbate is low, this model is reduced to the Freundlich model and when the concentration is high, the model predicts the monolayer adsorption capacity of the Langmuir isotherm. The operational conditions (pH, temperature, and concentration) affect the parameters of the equation of this isotherm mode [41,42]. The following formula presents the Sips isotherm model:

$$q_e = \frac{K_s C_e^\beta}{1 - a_s C_e^\beta} \quad (6)$$

Where K_s (1/Lg) and a_s (1/Lg) are Sips isotherm constants and β is Sips isotherm exponent[30].

Redlich-Peterson isotherm model

The three-parameter Redlich-Peterson model is the combination of the two models of Langmuir and Freundlich. This isotherm model has mixed elements from Langmuir and Freundlich equations and, therefore, follows the mechanism of mixed adsorption and cannot follow the ideal monolayer adsorption. In this model, in order to show the adsorption equilibrium over a wide range of pressure, there exists a linear dependence on the pressure value in the numerator and the denominator is an exponential function [30,43].

$$q = \frac{A C_e}{1 + B C_e^\beta} \quad (7)$$

Where A and B are Redlich-Peterson isotherm constants ($1/Lg$), C_e is equilibrium liquid-phase concentration of the adsorbent (mg/L), β (an exponent which lies between 0 and 1), and q is equilibrium adsorbate loading on the adsorbent (mg/g) [30].

Dubinin-Astakhov isotherm model

The isotherm model of Dubinin-Astakhov is an experimental model which is used to model the adsorption equilibrium of a range of gases and vapors on heterogeneous carbon-based adsorbents. The model's performance relies on the mechanism of micro-pore volume filling. Three very important parameters in this model are:

- The characteristics energy (E),
- The limiting volumetric adsorbate uptake (q_0), and
- The adsorbent surface-structural heterogeneity parameter (n),

Which are estimated through linear regression analysis of the isotherm's data, to ensure the best fit [33,44]. The equation of Dubinin-Astakhov is presented here:

$$q = q_d \exp \left[K_{DA} \left(\ln \left(\frac{P}{P_0} \right) \right)^m \right] \quad (8)$$

Where q ($mmol/g$) is the amount of adsorbed CO_2 , q_d ($mmol/g$) is the isotherm's maximum capacity, P (kPa) is the equilibrium pressure of CO_2 , P_0 is the adsorbate saturation pressure (kPa), and K_{DA} is the constant of the Dubinin-Astakhov model. In addition, R , T , and E are the universal gas constant ($8.314 J/mol.K$), the absolute temperature (K), the isothermal work (J/mol) needed to compress the gas from the pressure of equilibrium (P) to its saturation pressure, (P_0), respectively [29].

Error analysis

In this study, following the common approach in previous studies, the Average Relative Error (ARE) was applied to find the model which has been had the best fitting with the experimental isotherm data [44,45]. This function aims to minimize the distribution of fractional error and its formula is:

$$ARE = \frac{100}{n} \sum_{i=1}^n \left| \frac{q_{meas} - q_{calc}}{q_{meas}} \right|_i \quad (9)$$

Where n is the number of experimental data, q_{meas} ($mmol/g$) is the amount of CO_2 measured, and q_{calc} ($mmol/g$) is the amount of adsorbed calculated using the isotherm model[29].

Henry's law constant (adsorption affinity evaluation)

Henry's law constant is an essential parameter in adsorption studies, which shows the attraction of the adsorbate to the adsorbent[46]. This value is determined by calculating the slope of the adsorption isotherm at zero load. The constant is shown below[29]:

$$K_H = \lim_{P \rightarrow 0} \left(\frac{q}{P} \right) = \lim_{P \rightarrow 0} \left(\frac{dq}{dP} \right) \quad (10)$$

Where K_H ($mmol/gKPa$) is Henry's law constant and q ($mmol/g$) is the adsorption capacity loading [29].

In this study, to estimate Henry's law constant for the adsorption of CO_2 on pumice, the Virial model was used, because of the high level of accuracy, it can grant. It can be seen below:

$$\frac{p}{q} = \frac{1}{K_H} \exp \left(2A_1q + \frac{3}{2}A_2q^2 + A_3q^3 + \dots \right) \quad (11)$$

Where A_1, A_2, A_3 , are the virial model coefficient. A plot of $\ln(p/q)$ versus q represents the axis linearly with slope $2A_1$ and intercept $-\ln(K_H)$ [29].

EXPERIMENTAL SECTION

Adsorbent characteristics

In this study, for the first time, pumice rock (Gharveh mine in Iran) was used as an adsorbent. The pumice surface was modified with the chemical compound tetraethylenepentamine (TEPA). To evaluate the structure of pumice was used X-Ray Diffraction (Philips-Xpert Pro) device in the XRD test. To measure the amount of adsorption and desorption, liquid nitrogen at 77 K (BET test) was used along with the Microtrace Belsorb Mini II device at the preparation conditions of 120 degrees Celsius. Also, to examine the surface and microstructure of inner layers of pumice at the micro- and nano-dimensions, the Scanning electron microscope SEM (LEO1450 UP) was used. Moreover, the Perkin-Elmer Spectrum one FT-IR spectrophotometer was used to examine the molecule structure, and to identify carbon compounds and modifier groups. The capacity of pure CO_2 adsorption on the three samples of raw adsorbent (natural)

was studied using Microtrac Belsorp-max (Made in Japan).

Modification of pumice surface with the chemical compound of (TEPA)

In 2003, Xu et al. offered a method for the modification of the surface of silica adsorbents using amine compounds (Tetraethylenepentamine), which became common [47, 48]. Although pumice contains SiO₂ (more than 50%), because of its natural structure, the common method cannot be used to make bonds between its surface and amine compounds. Thus, in this study, a new synthesis method is presented. In this method, 0.01 moles of 2-(3,4-Epoxy cyclohexyl) ethyltriethoxysilane equal to 2.88 grams (to improve adhesion) and 0.01 moles of Tetraethylenepentamine equal to 1.89 grams were mixed inside 50 cc beaker containing 10 mL of isopropyl amine with Oxirene. The solution was added at a weight percent of 6, as the modifier of pumice. The method involved adding three 10-gram samples of pumice powder were put in three different containers, then 10 milliliters of the solution of water and ethanol at 1:10 volume percent was added and the modifier at the mentioned percentages was added to the beaker while the mixture was being stirred. The content of the beaker was in contact and stirred with ammonia (0.01%) for one hour at the temperature of 60 degrees Celsius. The sediments were poured on filter paper and were washed by 60% ethanol three times and were completely dried in a vacuum oven for 4 hours at 60 degrees Celsius.

Determination of CO₂ adsorption capacity

At first, the capacity of pure CO₂ adsorption on the sample of raw adsorbent (Pumice) was studied using the Belsorp-max device. Adsorption isotherms were measured at the pressure range of 0 to 1 (Bar) and 298K. The purity of CO₂ was 99.99%. The adsorption capacity of Pumice modified by 6% TEPA, according to the variable temperatures in the flue gas from industries, was measured at 298, 328, and 348K.

Equilibrium isotherms

To determine the best-fit isotherm, the experimental equilibrium data were analyzed by eight adsorption isotherm models with two and three parameters. Two-parameter isotherms used in this study were included, the Langmuir, Freundlich, BET,

and Temkin and three-parameter isotherms were including, the Redlich-Peterson, Sips, Toth, and Dubinin-Astakhov.

Error functions

The Average Relative Error (ARE) was applied to find the model which had the best fitting with the experimental isotherm data.

The adsorbent's Cost index

The adsorbent's Cost index was calculated through Eq. (12) [49].

$$\text{Adsorbent cost} = \frac{[\text{Chemical purchase cost (US\$)} + \text{Energy cost (US\$)}]}{\text{Adsorbent capacity (mmol/g)}} \quad (12)$$

RESULTS AND DISCUSSION

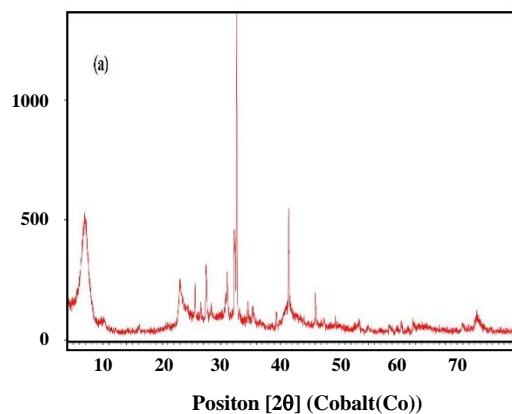
The chemical properties of Pumice are presented in Table (1). The constituents of natural pumice are most often silica (SiO₂) and aluminum oxide (Al₂O₃), with values of 54.51 and 16.42 percent, respectively.

The results of the sample pumice's XRD test are shown in Fig. 1. In these results, which belong to pumice from Maragheh, the crystal phase can be seen when $2\theta = 23, 25.5, 28.5, 31, 32.5, 33, \text{ and } 41.5$ [23]. The sample contains crystals such as quartz and albite.

The FT-IR spectrum provides us with information on functional groups, their molecular geometry, and intermolecular reactions. In Fig. 2, the FT-IR spectrum for pumice is shown. The wavelengths are between 500 and 4000 cm⁻¹. In this sample, the wavelengths of 1033 cm⁻¹, 1037 cm⁻¹, 1048 cm⁻¹, 461 cm⁻¹, and 780 cm⁻¹ are related to the characteristics of SiO₄ group and the reason for them is the symmetric stretching vibration in Si-O-Si. In other words, the wavelengths indicate the bond between silicon and oxygen compounds. The wavelengths of 3479 cm⁻¹, 3478 cm⁻¹, and 3633 cm⁻¹ are related to the H-OH-OH bonds. The bending vibration of H-O is shown in 1639 cm⁻¹ and 1641 cm⁻¹ wavelengths [50-53]. The pumice modified with TEPA (6%) exhibited changes in the wavelengths of 2000–4000 cm⁻¹, but no wavelengths representing the composite band between oxygen and silica were changed.

Table 1: The chemical properties of Pumice

Elements	SiO ₂	Al ₂ O ₃	CaO	MgO	TiO ₂	Fe ₂ O ₃	MnO	SO ₃	P ₂ O ₅	Na ₂ O	K ₂ O	SrO	ZnO	Cl
Unit (%)	54.51	16.42	3.48	2.54	0.37	3.32	<0.1	<0.1	0.11	0.69	1.15	<0.1	<0.1	<0.1

**Fig 1: XRD pattern of natural pumice stone.**

The morphology of pumice was observed by a Scanning Electron Microscope (SEM) and is given in Fig. 3. In the pumice sample from Maragheh, the amorphous structure of lamella is divided into uneven phases and bonds, which reveals the extruded nature of matters with evenly spread pores [54].

The BET results of powdered pumice in the sample from Maragheh's pumice mine were acceptable, and this was approved in the adsorption test too. In general, after grinding, the specific surface area increased from 40.426 m²/g to 45.947 m²/g. However, the amount of porosity decreased from 0.1179 cm³/g to 0.0198 cm³/g. As is shown in Fig. 4, the sizes of pumice particles before and after grinding are 150 and 20 μm respectively.

According to the results of the study, at the temperature of 298 K, modified pumice demonstrated better adsorption. Its adsorption capacity (0.510 mmol/g) was almost twice as much as that of raw pumice. In comparison to some of the modified mineral adsorbents like Kaolinite and Bentonite, with adsorption capacities of 0.068 mmol/g and 0.204 mmol/g, respectively, and also ZSM5, with the adsorption capacity of 0.159 mmol/g, the adsorption capacity of pumice was higher than that adsorption capacity [55]. The capacities of Bentonitic materials on which surface was modified with acid in four samples of M1f, M4f, M4f-3, and M4f-6 were 0.28 mmol/g, 0.244 mmol/g, 0.431 mmol/g, and 0.445 mmol/g,

respectively [56]. All of the adsorption capacities are lower than the amount estimated in this study.

Fig. 5, compares the results for CO₂ adsorption between raw pumice at 298K and amine-modified pumice at three different temperatures. Table 2 presents the statistical correspondence between the experimental data on the adsorption of CO₂ on modified pumice at three different temperatures of 298K, 328K, and 348K, in terms of their two- and three-parameter isotherm models and the estimations of Average Relative Error (ARE).

Using the theoretical q_{max}, the results indicated that from among the three-parameter isotherm models, the Sips model at 298K and 328K enjoyed the closest correspondence with the experimental data. The Sips model's value at 348K was also reasonable.

In addition, among the two-parameter models, the Freundlich model yielded acceptable results in relation to the experimental data. It could be concluded that CO₂ is in contact with the heterogeneous surface of pumice, which provides uniform distribution of the adsorption energy. In general, three-parameter isotherms showed better correspondence with experimental data on the adsorption of CO₂, in comparison with two-parameter equilibrium isotherms.

In Langmuir isotherm, K_L (1/KPa) is the constant of the model and shows the adsorption energy and the tendency of gas molecules to be adsorbed on the adsorbent. The less this constant is, the less the amount of maximum adsorption of gas molecules on the adsorbent will be [31]. Based on the results, the amount of K_L at the three temperatures of 298K, 328K, and 348K was 7.45, 3.97, and 3.92 (1/KPa), respectively. As the constant decreased at higher temperatures, the capacity of CO₂ adsorption on pumice also went down.

The Freundlich constants are K_F (mmol/g atm^{1/n}), which indicates the adsorption capacity, and n, which is the heterogeneity factor. A high value for n_F = 1/n results in higher adsorption capability, as well as higher heterogeneity degree [32]. If K_F falls between 0-20, adsorption could be promising. The current study showed that K_F at three different temperatures equaled 3.20, 2.51,

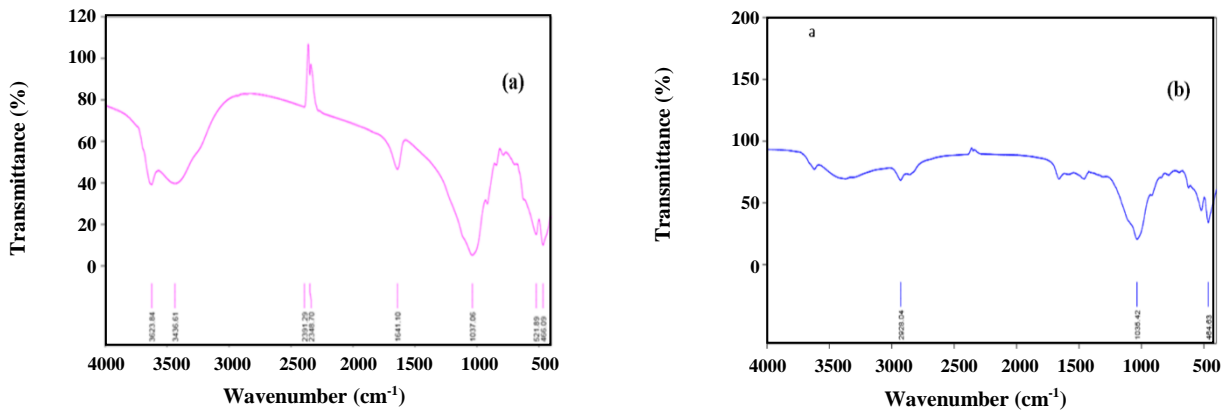


Fig. 2: FTIR spectrum of the natural pumice (a), pumice modified (b).

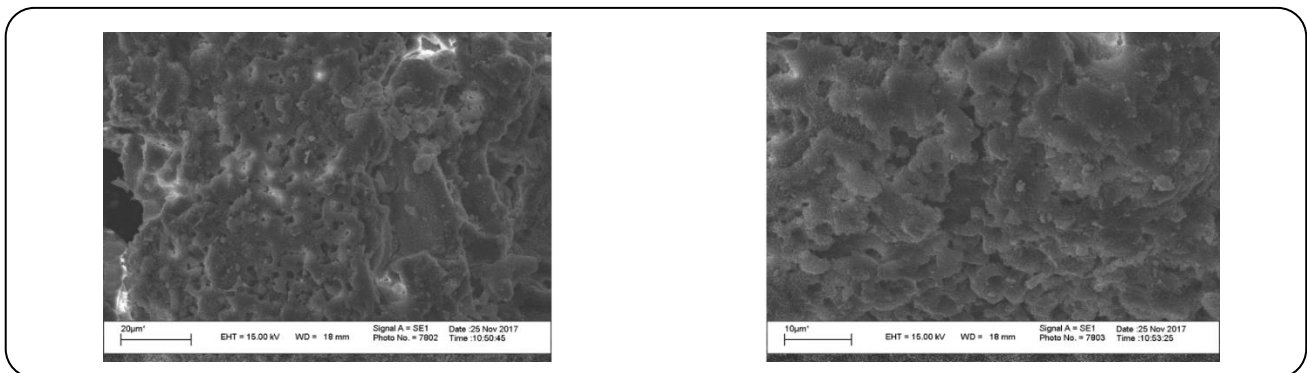


Fig. 3: SEM photomicrographs of natural pumice.

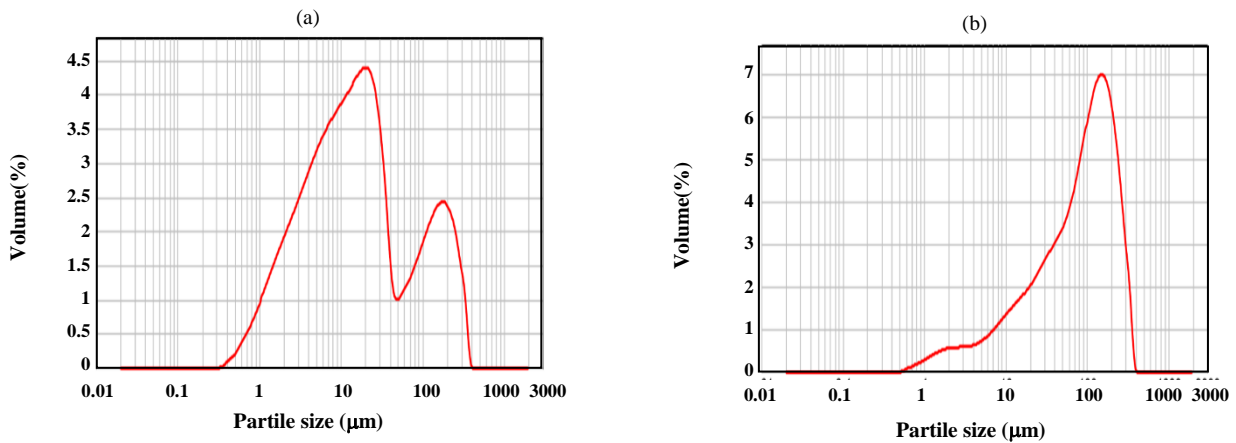


Fig. 4: Pumice particles 'size before grinding (a) pumice particles 'size after grinding (b).

and 2.38 ($\text{mmol/g atm}^{1/n}$), respectively. If the amount of n is above 1, it shows that the model is suitable for the adsorption, and as it is seen in Table (2), the amount of n at all three temperatures was above 1.

The results regarding BET model at 328K and 348K were disappointing, so the model was ignored. In Temkin isotherm, the assumption is that if the adsorption sites

increase, the gas is adsorbed in a linear manner. Temkin isotherm equilibrium binding constant (K_T) provides us with information about binding energy. According to the findings, at 298K, the highest amount was yielded.

q is the maximum adsorption capacity in the Toth model and is estimated to be at its highest at 298K (14.5 mmol/g). t is an estimation for the adsorbent's heterogeneity.

Table 2: Comparison of two-parameter and three-parameter isotherms for different temperatures

Tow- parameter isotherm	298K	328K	348K	Three- parameter isotherm	298K	328K	348K
Langmuir				Redlich-Peterson			
q_{\max}	0.529	0.481	0.427	A	46025.5	7864.2	8.948
K_L	7.453	3.975	3.920	B	46.419	19405	24.176
(ARE)%	9.429	6.025	10.196	β	0.483	0.602	0.642
Freundlich				(ARE)%	4.232	0.336	8.67
K_f	0.495	0.405	0.359	Sips			
N	3.201	2.515	2.383	K_S	0.097	0.414	0.536
(ARE)%	2.507	0.336	5.314	B	0.080	0.403	0.537
Temkin				a_s	0.807	-0.022	-0.516
b_T	26003	26257	36929	(ARE)%	0.341	0.357	2.47
A_T	144.82	57.59	125.31	Toth			
(ARE)%	56.60	56.80	60	q_s	14.526	10.084	4.549
BET				K_T	9450	55.507	21/109
q_b	0.518			T	0.0996	0.1399	0.179
K_B	498.87			(ARE)%	3.275	1.076	1.637
(ARE)%	9.21			D-A			
				q_d	1401.2	2.019	
				K_{DA}	5.982	0.374	
				M	0.198	1.022	
				(ARE)%	250	216	

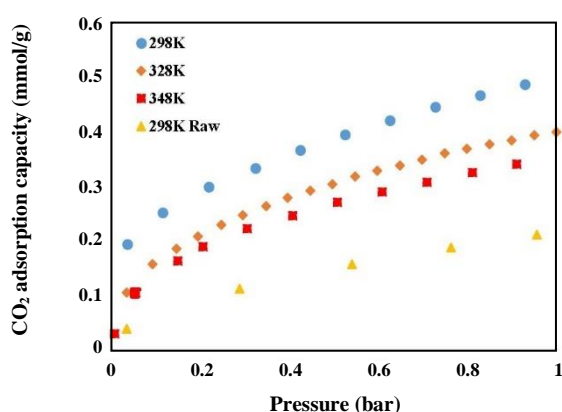


Fig. 5: comparison of the results for CO_2 adsorption between raw pumice at 298K and amine-modified pumice at 298K, 328K, and 348K.

The magnitude of the heterogeneity of the adsorbent shows the mobility of and interactions between the adsorbed gas molecules on the adsorbent. It also accounts for the binding tendency of the adsorption sites to adsorb the molecules of the target gas [42]. The results of this study showed a value less than 1 for t at all three temperatures.

The maximum adsorption capacity in the Sips isotherm model at 348K was estimated. If the heterogeneity factor ($1/n$) is less than or equal to 1, it is concluded that the surface is homogeneous. In D-A model, if the fitting parameter's value is less than 2 ($m < 2$), the gas molecules are adsorbed on a heterogeneous adsorbent. Based on this model, the isothermal work (E) is defined in terms of the work which is required for compressing gas from its

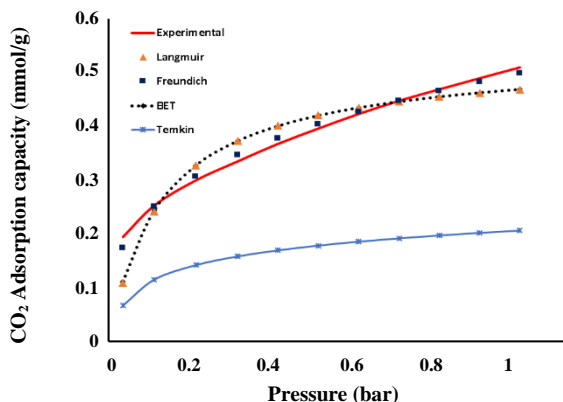


Fig. 6: Nonlinear fit of 2 parameters models to the experimental CO_2 equilibrium data of modified Pumice adsorbent in 298K.

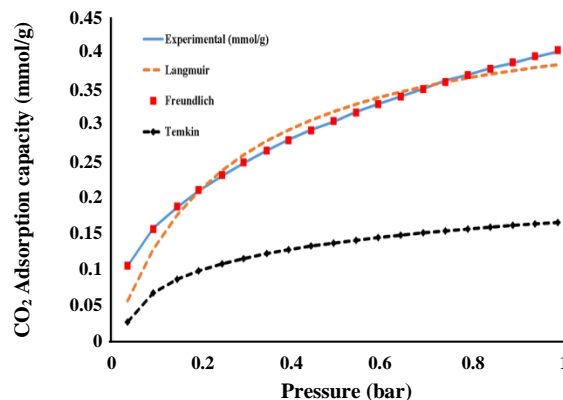


Fig. 8: Nonlinear fit of 2 parameters models to the experimental CO_2 equilibrium data of Modified Pumice adsorbent in 328K.

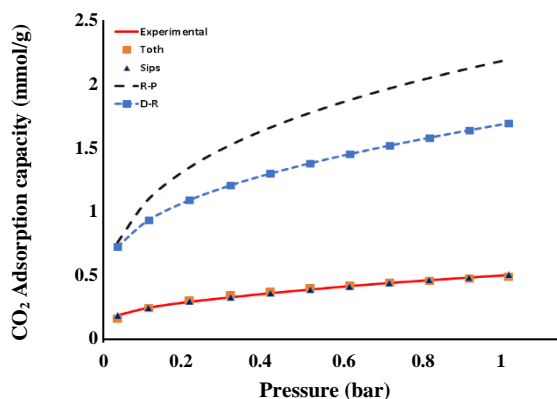


Fig. 7: Nonlinear fit of 3 parameters models to the experimental CO_2 equilibrium data of modified Pumice adsorbent in 298K.

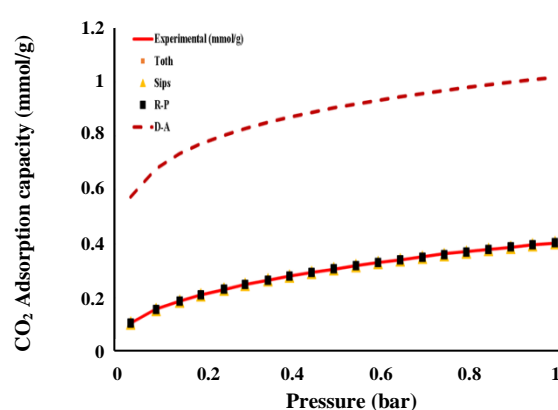


Fig. 9: Nonlinear fit of 3 parameters models to the experimental CO_2 equilibrium data of modified Pumice adsorbent in 328K.

equilibrium pressure (P) to the saturation pressure (P_0). The results suggest that the amount of E at 298K and 328K was lower than 8, which signals the domination of the adsorption mechanism in the process of CO_2 adsorption on modified pumice [32, 42]. However, at 348K, the value of E was estimated to be 12.402 (kJ/mol), which implies that other absorption mechanisms might be at work as well. It should be noted that at 348K, the three-parameter D-A model was not favorable, so they were ignored.

The results of the fitting of experimental data with the two- and three-parameter isotherm models at 298K, 328K, and 348K are shown in Figs. 6 to 11.

Examining the value of Henry's law constant in raw pumice 298K, in comparison with modified pumice at the three different temperatures, demonstrated that Henry's law constant was higher in the modified adsorbent than in the raw adsorbent.

The highest amount of Henry's law constant for modified pumice was at 298K, which was calculated to be around (13.59 mmol/g bar). Fig. 12, shows the correlation between temperature increase and Henry's law constant.

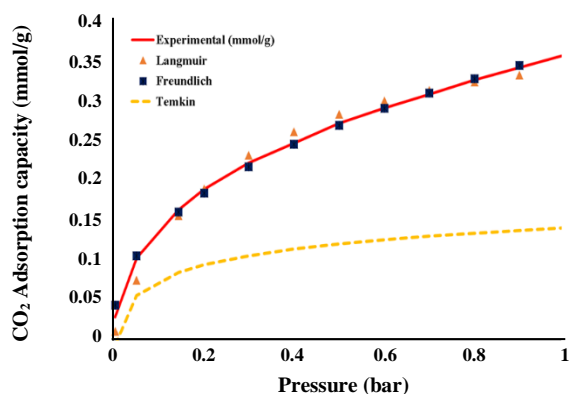
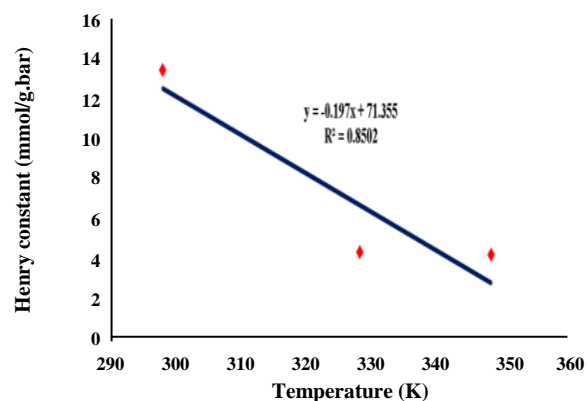
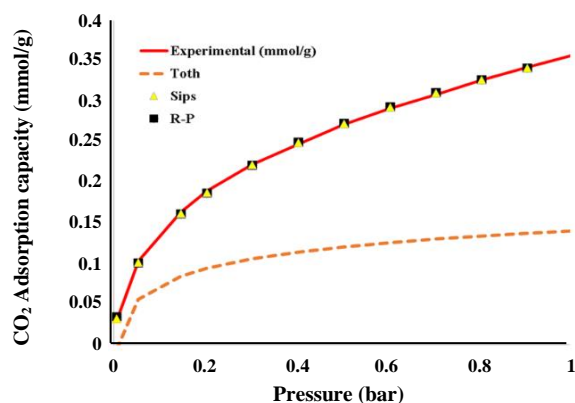
The results of error analysis, using the estimations of Average Relative Error (ARE), are given in Table 2. The results signify that from among two- and three-parameter isotherm models, the Freundlich model, and Sips model, at all three temperatures, showed closer correspondence with experimental data on CO_2 adsorption on modified pumice ($\text{ARE} < 3$). As it can be seen in Table 3, modified pumice's cost index is lower than those of other synthesized adsorbents.

CONCLUSIONS

In this study, the experimental data on CO_2 adsorption on natural pumice, and amine-modified pumice were compared.

Table 3: Comparison cost index between modified pumice and some synthesized adsorbents.

Adsorbent	Chemicals purchase cost (US\$)	Energy cost (US\$)	CO ₂ adsorbent capacity (mmol/g)	Adsorbent preparation cost (US\$/mmol/g)	Ref.
Fe ₃ O ₄ -rGO	14.410	0.005	2.500	5.766	[57]
GO-UiO-66	29.679	0.032	3.370	8.818	[58]
GO-ZnO	21.663	0.032	1.940	11.183	[59]
N-doped rGO-Zn	43.048	0.308	3.310	13.098	[60]
Modified Pumice	1.48	0.015	0.51	2.93	This study

**Fig. 10: Nonlinear fit of 2 parameters models to the experimental CO₂ equilibrium data of modified Pumice adsorbent in 348K.****Fig. 12: Relationship between increasing temperature and Henry's low constant.****Fig. 11: Nonlinear fit of 3 parameters models to the experimental CO₂ equilibrium data of modified Pumice adsorbent in 348K.**

In addition, the results were examined using 8 isotherm models and error analysis.

According to the results, the adsorption capacity in amine-modified pumice was twice as much as that of raw pumice. It proves the effect of TEPA coverage on the surface on the better performance of the adsorbent.

The Freundlich model, in comparison with the other two-parameter models, and the Sips model, compared to the other three-parameter models, showed the best correspondence with CO₂ adsorption's experimental data. Overall, the results indicated that three-parameter models had closer correspondence with experimental data than their two-parameter counterparts did. The CO₂ adsorption capacity on modified pumice at 298K was higher than the capacity at 328K and 348K. It means the adsorbent performs better at lower temperatures. Additionally, the amount of E (kJ/mol) implies the domination of the physical adsorption mechanism in the process.

Based on Henry's law constant, CO₂ at 298K is most likely to be adsorbed on modified pumice adsorbent. It approves the experimental findings of the adsorption capacity.

One of the important factors in the commercialization and industrial applications of any sorbent is the absorption cost index, which includes the price of chemicals and the energy required to manufacture it. Although research on CO₂ adsorption capacity obtained from amine-modified

pumice adsorbent (0.510 mmol/g) is lower than some synthesized adsorbents, the cost of manufacturing this adsorbent was negligible compared to other adsorbents that justify its commercial use.

Received : Dec. 3, 2019 ; Accepted : May 4, 2020

REFERENCES

- [1] Sánchez-Zambrano K.S., Lima Duarte L., Soares Maia D.A., Vilarrasa-García E., Bastos-Neto M., Rodríguez-Castellón E., Silva de Azevedo D.C., [CO₂ Capture with Mesoporous Silicas Modified with Amines by Double Functionalization: Assessment of Adsorption/Desorption Cycles](#), *Materials*, **11**(6): 887-906 (2018).
- [2] Noorpoor A., Nazari Kudahi S., Mahmoodi N.M., [Adsorption Performance Indicator for Power Plant CO₂ Capture on Graphene Oxide/TiO₂ Nanocomposite](#). *Iranian Journal of Chemistry and Chemical Engineering (IJCCE)*, **38**(3): 293-307 (2019).
- [3] Anas M., Anas M., Gönel A.G., Bozbag S.E., Erkey C., [Thermodynamics of Adsorption of Carbon Dioxide on Various Aerogels](#), *CO₂ Utilization*, **21**: 82-88 (2017).
- [4] Guarín Romero J.R., Moreno-Piraján J.C., Giraldo Gutierrez L., [Kinetic and Equilibrium Study of the Adsorption of CO₂ in Ultramicropores of Resorcinol-Formaldehyde Aerogels Obtained in Acidic and Basic Medium](#), *Carbon Research* **4**(4): 52-71 (2018).
- [5] Ma Y., Wang Z., Xu X., Wang J., [Review on Porous Nanomaterials for Adsorption and Photocatalytic Conversion of CO₂](#), *Chinese Journal of Catalysis*, **38**(12): 1956-1969 (2017).
- [6] Cuéllar-Franca R.M., Azapagic A., [Carbon Capture, Storage and Utilisation Technologies: A Critical Analysis and Comparison of their Life Cycle Environmental Impacts](#), *CO₂ utilization*, **9**: 82-102 (2015).
- [7] Asif M., Suleman M., Haq I., Jamal S.A., [Post-Combustion CO₂ Capture with Chemical Absorption and Hybrid System: Current Status and Challenges](#), *Greenhouse Gases: Science and Technology*, **8**(6): 998-1031 (2018).
- [8] Li T., Keener T.C., [A review: Desorption of CO₂ from Rich Solutions in Chemical Absorption Processes](#), *Greenhouse Gas Control*, **51**: 290-304 (2016).
- [9] Ben-Mansour R. Qasem N.A., [An Efficient Temperature Swing Adsorption \(TSA\) Process for Separating CO₂ from CO₂/N₂ Mixture Using Mg-MOF-74](#), *Energy Conversion and Management*, **156**: 10-24 (2018).
- [10] Ouyang, J., Zheng C., Gu W., Zhang Y., Yang H., Suib S.L., [Textural Properties Determined CO₂ Capture of Tetraethylenepentamine Loaded SiO₂ Nanowires from \$\alpha\$ -Sepiolite](#), *Chemical Engineering*, **337**: 342-350 (2018).
- [11] Norahim N., Yaisanga P., Faungnawakij K., Charinpanitkul T., Klaysom C., [Recent Membrane Developments for CO₂ Separation and Capture](#), *Chemical Engineering & Technology*, **41**(2): 211-223 (2018).
- [12] Míguez J.L., Porteiro J., Pérez-Orozco R., Gómez M. Á., [Technology Evolution in Membrane-Based CCS](#), *Energies*, **11**(11): 3153-3171 (2018).
- [13] Wdowin M., Tarkowski R., Franus W., [Determination of Changes in the Reservoir and Cap Rocks of the Chabowo Anticline Caused by CO₂-Brine-Rock Interactions](#), *Coal Geology*, **130**: 79-88 (2014).
- [14] Yaumi A., Bakar M.A., Hameed B., [Melamine-Nitrogenated Mesoporous Activated Carbon Derived from Rice Husk for Carbon Dioxide Adsorption in Fixed-Bed](#), *Energy*, **155**: 46-55 (2018).
- [15] Li S., Deng S., Zhao L., Zhao R., Lin M., Du Y., Lian Y., [Mathematical Modeling and Numerical Investigation of Carbon Capture by Adsorption: Literature Review and Case Study](#), *Applied Energy*, **221**: 437-449 (2018).
- [16] Alfe M., Ammendola P., Gargiulo V., Raganati F., Chirone R., [Magnetite loaded Carbon Fine Particles as Low-Cost CO₂ Adsorbent in a Sound Assisted Fluidized Bed](#), *Proceedings of the Combustion Institute*, **35**(3): 2801-2809 (2015).
- [17] Patel H.A., Byun J., Yavuz C.T., [Carbon Dioxide Capture Adsorbents: Chemistry and Methods](#), *ChemSusChem*, **10**(7): 1303-1317 (2017).
- [18] Çiçi D.İ., Meriç S., [A Review on Pumice for Water and Wastewater Treatment](#), *Desalination and Water Treatment*, **57**(39): 18131-18143 (2016).
- [19] Turan N., Akdemir A., Ergun O., [Removal of Volatile Organic Compounds by Natural Materials During Composting of Poultry Litter](#), *Bioresource Technology*, **100**(2): 798- 803 (2009).

- [20] Samarghandi M.R., Samarghandi M.R., Daraee Z., Shekher Giri B., Asgari G., Reza Rahmani A., Poormohammadi A., [Catalytic Ozonation of Ethyl Benzene Using Modified Pumice with Magnesium Nitrate from Polluted Air](#), *Environmental Studies*, **74(3)**: 486-499 (2017).
- [21] Mboya, H.A., Mboya H.A., King'onde C.K., Njau K.N., Mrema A.L. , [Measurement of Pozzolan Activity Index of Scoria, Pumice, and Rice Husk Ash as Potential Supplementary Cementitious Materials for Portland Cement](#), *Advances in Civil Engineering*, **2017(2)**:1-13 (2017).
- [22] Hahn M.W., Jelic J., Berger E., Reuter K., Jentys A, Lercher J.A., [Role of Amine Functionality for CO₂ Chemisorption on Silica](#), *Physical Chemistry B*, **120(8)**: 1988-1995 (2016).
- [23] Ojeda M., Mazaj M., Garcia S., Xuan J., Maroto-Valer M.M., Logar N.Z., [Novel Amine-Impregnated Mesoporous Silica Materials for CO₂ Capture](#), *Energy Procedia*, **114**: 2252-2258 (2017).
- [24] Fakhroeslam M., Fatemi S., [Comparative Simulation Study of PSA, VSA, and TSA Processes for Purification of Methane from CO₂ via SAPO-34 Core-Shell Adsorbent](#), *Separation Science and Technology*, **51(14)**: 2326-2338 (2016).
- [25] Mehdipour M., Fatemi S., [Modeling of a PSA-TSA Process for Separation of CH₄ from C₂ Products of OCM Reaction](#), *Separation Science and Technology*, **47(8)**: 1199-1212 (2012).
- [26] Beck J., Friedrich D., Brandani S., Guillas S., Fraga E.S., [Surrogate Based Optimisation for Design of Pressure Swing Adsorption Systems](#), *Computer-Aided Chemical Engineering, Elsevier.*, **30**:1217-1221 (2012).
- [27] Ambrozek B., "The Simulation of Cyclic Thermal Swing Adsorption (TSA) Process, in *Modelling Dynamics in Processes and Systems*", Springer, 165-178 (2009).
- [28] Karbalaeei Mohammad N., Ghaemi A., Tahvildari K., Sharif A.A.M., [Experimental Investigation and Modeling of CO₂ Adsorption Using Modified Activated Carbon](#), *Iranian Journal of Chemistry and Chemical Engineering (IJCCCE)*, **39(1)**:177-192 (2020).
- [29] Goel C., Kaur H., Bhunia H., Bajpai P.K., [Carbon Dioxide Adsorption on Nitrogen Enriched Carbon Adsorbents: Experimental, Kinetics, Isothermal and Thermodynamic Studies](#), *Journal of CO₂ Utilization*, **16**: 50-63 (2016).
- [30] Serafin J., Narkiewicz U., Morawski A.W., Wróbel R.J., Michalkiewicz B., [Highly Microporous Activated Carbons from Biomass for CO₂ Capture and Effective Micropores at Different Conditions](#), *Journal of CO₂ Utilization*, **18**: 73-79 (2017).
- [31] Noorpoor A., Kudahi S.N., [Analysis and Study of CO₂ Adsorption on UiO-66/Graphene Oxide Composite Using Equilibrium Modeling and Ideal Adsorption Solution Theory \(IAST\)](#), *Environmental Chemical Engineering*, **4(1)**: 1081-1091 (2016)
- [32] Ayawei N., Ebelegi A.N., Wankasi D., [Modelling and Interpretation of Adsorption Isotherms](#), *Chemistry*, 1-11, (2017).
- [33] Chen X., [Modeling of Experimental Adsorption Isotherm Data](#), *Information*, **6(1)**: 14-22 (2015).
- [34] Adelodun A.A., Ngila J. C., Kim D. G., Jo Y.M., [Isotherm, Thermodynamic and Kinetic Studies of Selective CO₂ Adsorption on Chemically Modified Carbon Surfaces](#), *Aerosol Air Qual. Res.*, **16**: 3312-3329 (2016).
- [35] Singh V.K., Kumar E.A., [Measurement and Analysis of Adsorption Isotherms of CO₂ on Activated Carbon](#), *Applied Thermal Engineering*, **97**: 77-86 (2016).
- [36] Rashidi N.A., Yusup S., Borhan A., [Isotherm and Thermodynamic Analysis of Carbon Dioxide on Activated Carbon](#), *Procedia Engineering*, **148**: 630-637 (2016).
- [37] Chowdhury S., Parshetti G.K., Balasubramanian R., [Post-combustion CO₂ Capture Using Mesoporous TiO₂/Graphene Oxide Nanocomposites](#), *Chemical Engineering*, **263**: 374-384 (2015).
- [38] Langmuir I., [The Adsorption of Gases on Plane Surfaces of Glass, Mica and Platinum](#), *The American Chemical Society*, **40(9)**: 1361-1403 (1918).
- [39] Raganati F., Alfe M., Gargiulo V., Chirone R., Ammendola P., [Isotherms and Thermodynamics of CO₂ Adsorption on a Novel Carbon-Magnetite Composite Sorbent](#), *Chemical Engineering Research and Design*, **134**: 540-552 (2018).
- [40] McKay G., Mesdaghinia A., Nasserli S., Hadi M., Aminabad M. S., [Optimum Isotherms of Dyes Sorption by Activated Carbon: Fractional Theoretical Capacity & Error Analysis](#), *Chemical Engineering*, **251**: 236-247 (2014).

- [41] Jedli H., Jbara A., Hedfi H., Bouzgarrou S., Slimi K., Carbon Dioxide Adsorption Isotherm Study on Various Cap Rocks in a Batch Reactor for CO₂ Sequestration Processes, *Applied Clay Science*, **136**: 199-207(2017).
- [42] Goel C., Bhunia H., Bajpai P.K., Novel Nitrogen Enriched Porous Carbon Adsorbents for CO₂ Capture: Breakthrough Adsorption Study, *Journal of Environmental Chemical Engineering*, **4**(1): 346-356 (2016).
- [43] Rostami A., Anbaz M.A., Gahrooei H.R.E., Arabloo M., Bahadori A., Accurate Estimation of CO₂ Adsorption on Activated Carbon with Multi-Layer Feed-Forward Neural Network (MLFNN) Algorithm, *Egyptian Journal of Petroleum*, **27**(1):65-73(2018).
- [44] Peyravi M., Synthesis of Nitrogen Doped Activated Carbon/Polyaniline Material for CO₂ Adsorption, *Polymers for Advanced Technologies*, **29**(1): 319-328 (2018).
- [45] Abunowara M., Bustam M.A., Sufian S., Eldemerdash U., Description of carbon dioxide adsorption and desorption onto Malaysian Coals under Subcritical Condition, *Procedia engineering*, **148**: 600-608 (2016).
- [46] Ngakou C.S., Anagho G.S., Ngomo H.M., Non-linear Regression Analysis for the Adsorption Kinetics and Equilibrium Isotherm of Phenacetin onto Activated Carbons, *Current Journal of Applied Science and Technology*, **36**: 1-18 (2019)
- [47] Sreńscek-Nazzal J., Narkiewicz U., Morawski A.W., Wróbel R.J., Michalkiewicz B., Comparison of Optimized Isotherm Models and Error Functions for Carbon Dioxide Adsorption on Activated Carbon, *Chemical & Engineering Data*, **60**(11): 3148-3158 (2015).
- [48] Prasetyo L., Do D., Nicholson D., A coherent definition of Henry Constant and Isotheric Heat at Zero Loading for Adsorption in Solids—An Absolute Accessible Volume, *Chemical Engineering*, **334**: 143-152 (2018).
- [49] Huong P.-T., Lee B.-K., Kim J., Improved Removal of 2-chlorophenol by a Synthesized Cu-Nano Zeolite, *Process Safety and Environmental Protection*, **100**: 272-280 (2016).
- [50] Chen C., Bhattacharjee S., Mesoporous Silica Impregnated with Organoamines for Post-Combustion CO₂ Capture: a Comparison of Introduced Amine Types, *Greenhouse Gases: Science and Technology*, **7**(6): 1116-1125 (2017).
- [51] Malakootian M., Bahraini S., Malakootian M., Removal of Tetracycline Antibiotic from Aqueous Solutions Using Natural and Modified Pumice with Magnesium Chloride, *Advances in Environmental Biology*, **10**: 46-56 (2016).
- [52] Mourhly A., Khachani M., Hamidi A.E., Kacimi M., Halim M., Arsalane S., The Synthesis and Characterization of Low-Cost Mesoporous Silica SiO₂ from Local Pumice Rock, *Nanomaterials and Nanotechnology*, **5**(35):1-7 (2015).
- [53] Guler U.A., Sarioglu M., Removal of Tetracycline from Wastewater Using Pumice Stone: Equilibrium, Kinetic and Thermodynamic Studies, *Environmental Health Science and Engineering*, **12**(1): 1- 11 (2014).
- [54] Parker R., Quantitative Determination of Analcime in Pumice Samples by X-Ray Diffraction, *Mineralogical Magazine*, **42**(321): 103-106 (1978).
- [55] Chouikhi N., Cecilia J.A., Vilarrasa-García E., Besghaier S., Chlendi M., Franco Duro F.I., Bagane M., CO₂ Adsorption of Materials Synthesized from Clay Minerals: A Review, *Minerals*, **9**(9):514- 536 (2019).
- [56] Venaruzzo J., Volzone C., Rueda M.L., Ortega J., Modified Bentonitic Clay Minerals as Adsorbents of CO, CO₂ and SO₂ Gases, *Microporous and Mesoporous Materials*, **56**(1): 73-80 (2002).
- [57] Zhou D., Liu Q., Cheng Q., Zhao Y., Cui Y., Wang T., Han B., Graphene-Manganese Oxide Hybrid Porous Material and Its Application in Carbon Dioxide Adsorption, *Chinese Science Bulletin*, **57**(23): 3059-3064 (2012).
- [58] Cao Y., Zhao Y., Lv Z., Song F., Zhong Q., Preparation and Enhanced CO₂ Adsorption Capacity of UiO-66/Graphene Oxide Composites, *Industrial and Engineering Chemistry*, **27**: 102-107 (2015).
- [59] Li W., Jiang X., Yang H., Liu Q., Solvothermal Synthesis and Enhanced CO₂ Adsorption Ability of Mesoporous Graphene Oxide-ZnO Nanocomposite, *Applied Surface Science*, **356**: 812-816 (2015).
- [60] Li W., Yang H., Jiang X., & Liu Q., Highly Selective CO₂ Adsorption of ZnO Based N-Doped Reduced Graphene Oxide Porous Nanomaterial, *Applied Surface Science*, **360**: 143-147 (2016).